Published in final edited form as:
J Environ Sci Health A Tox Hazard Subst Environ Eng. 2012 ; 47(2): 308–318. doi: 10.1080/10934529.2012.640911

A Generalized Model for Transport of Contaminants in Soil by Electric Fields

Juan M. Paz-Garcia[1,2], **Kitae Baek**[1,3], **Iyad D. Alshawabkeh**[4], and **Akram N. Alshawabkeh**[1]

[1]Department of Civil and Environmental Engineering, Northeastern University

[2]Department of Civil Engineering, Technical University of Denmark

[3]Department of Environmental Engineering, Kumoh National Institute of Technology

[4]Department of Chemistry, Jerash University, Jordan

Abstract

A generalized model applicable to soils contaminated with multiple species under enhanced boundary conditions during treatment by electric fields is presented. The partial differential equations describing species transport are developed by applying the law of mass conservation to their fluxes. Transport, due to migration, advection and diffusion, of each aqueous component and complex species are combined to produce one partial differential equation hat describes transport of the total analytical concentrations of component species which are the primary dependent variables. This transport couples with geochemical reactions such as aqueous equilibrium, sorption, precipitation and dissolution. The enhanced model is used to simulate electrokinetic cleanup of lead and copper contaminants at an Army Firing Range. Acid enhancement is achieved by the use of adipic acid to neutralize the basic front produced for the cathode electrochemical reaction. The model is able to simulate enhanced application of the process by modifying the boundary conditions. The model showed that kinetics of geochemical reactions, such as metals dissolution/leaching and redox reactions might be significant for realistic prediction of enhanced electrokinetic extraction of metals in real world applications.

Keywords

Electrokinetic Remediation; Lead; Cupper; Mathematical Model; Reactive Transport

INTRODUCTION

A group of electrokinetic and electrochemical remediation technologies are developed to treat sites polluted with toxic heavy metals, radionuclides, and organic pollutants. The technologies are based on application of electric currents across electrodes inserted in the soil to induce electrolysis and generate an electric field. Ambient or introduced solutes migrate in response to the imposed electric field by electroosmosis and ionic migration. Electroosmosis mobilizes the pore fluid to flush solutes, usually toward the cathode, while ionic migration effectively separates anionic and cationic species, drawing them to the anode and cathode, respectively. This transport coupled with geochemical reactions, such as sorption, precipitation and dissolution, are the fundamental mechanisms of electrokinetic remediation. Contaminant extraction and removal are accomplished by electrodeposition, precipitation or ion exchange either at the electrodes or in an external extraction system.

Electrokinetic extraction of metals and radionuclides from soils has been investigated by bench-scale tests, pilot-scale tests, and limited field applications. [1-12] The major advantages of the technology include: (a) it can be implemented in situ with minimal

disruption, (b) it is well suited for fine-grained, heterogeneous media, where other techniques such as pump-and-treat can be ineffective, and (c) accelerated rates of contaminant transport and extraction may be obtained.

In electrokinetic extraction of metals, the electrical current applied is transformed to an ionic current in the pore solution by means of the electrochemical reactions taking place at the electrodes.

Electrode reactions can vary depending on the chemical species present in the media. Electrolysis of water reactions, oxidation at the anode (1) and reduction at the cathode (2), are always likely to occur, as follows,

$$H_2O \rightleftarrows \frac{1}{2}O_2 + 2H^+ + 2e^- \quad (1)$$

$$2H_2O + 2e^- \rightleftarrows H_2 + 2OH^- \quad (2)$$

Water electrolysis generates an acidic medium at the anode (1), which can decrease the pH to below 2, and an alkaline medium at the cathode (2), which may increase the pH to above 10 [7]. Proton (or hydronium ion, H_3O^+) mobility under electrical field is about twice that of the hydroxyl ion (OH^-) which results in a faster advance of the acid front relative to the base front [13]. Transport of the H_3O^+ is also enhanced by electroosmotic advection, which usually acts from the anode towards the cathode. In unamended treatments, strong pH changes are expected in the pore solution. Unless the transport of the proton is retarded by the soil buffering capacity [14], the soil between the electrodes will be acidified. This acidification results in enhanced solubilization of contaminants susceptible to cation exchange and dissolution at lower pH. Once contaminants are dissolved or complexed to an ionized solute, they migrate to the electrode of opposite polarity under the applied electric field leading to their extraction from the soil. Electrical neutrality of the pore fluid is maintained by transport of equivalent cations and anions in and out from a unit volume of pore fluid. Rigorous consideration of geochemical behavior is necessary due to the range of pH conditions and ion activity induced between the electrodes. Speciation, ion exchange, and dissolution-precipitation are among the reactions of potential significance. In unamended electrokinetic remediation, the protons that transport across the soil meet the hydroxyl ions close to the cathode compartment resulting in neutralization and the generation of water. A section with high pH gradient is formed, which can affect to the chemical speciation. Some metals are amphoteric, i.e., can exist either in positive or negative ion forms e.g., Pb^{2+} or $Pb(OH)_3^-$, Cr^{3+} or $Cr(OH)_4^-$ depending on the local conditions. A change in magnitude or polarity of the charge of a complex would affect the rate and direction of migration, conceivably to the stalling the advance of the contaminant in a pH gradient zone. Additionally, in the more alkaline region metal hydroxides precipitation may decrease the concentrations of the ionic species in the pore fluid, decreasing the electrolyte strength, and creating a zone of low electrical conductivity in the soil adjacent to the cathode. The formation of this low conductivity zone results in a significant increase in the voltage gradient across the soil and a commensurate increase in the energy expenditure required to mobilize ions.

Different schemes have been proposed to enhance transport and extraction of species under electric fields, and to prevent formation of precipitates. The objective of some of these schemes is to neutralize the cathode water electrolysis reaction to avoid generation and transport of high concentrations of the OH- ion into the soil and to enhance metal electrodeposition at the cathode. In these acid-enhanced treatments, the neutralization of the

cathode water electrolysis reaction will also assist in decreasing the electrical potential difference across the electrodes and consequently decrease energy expenditure. Acetic, sulfamic, and other acids could be introduced at the cathode at a controlled rate to prevent an increase in the catholyte pH [7; 10; 12]. Extracting agents are used in combination of the aforementioned acid enhancement, in order to obtain a soluble complex ion by chemical reaction between the target heavy metal and the extracting agent.

GENERALIZED MODELLING

Contaminant transport models which incorporate electrical gradients are limited [2; 15-20]. Shapiro et al. [2] and Shapiro and Probstein [15] developed a one-dimensional model for transport of chemical species under electrical gradients, incorporating the electrochemical processes, extended to a two-dimensional by [21]. The model couples the transport equations of N chemical species together with the charge flux equation and accounts for specific chemical reactions in the soil pore fluid. A steady-state electroosmotic flux is assumed and the comparisons with experimental results display good agreement with one case of acetic acid transport. This model, however, assumes incompressible soil medium, and disregards the changes in hydraulic potential distribution. Jacobs et al. [18] improved the Shapiro and Probstein [15] model by incorporating complexation and precipitation reactions. Haran et al. [20] presented a model for the transport of hexavalent chromium under electric fields in sand.

Electroosmotic flow is assumed zero as the model was implemented for a case of sandy soil. Acar et al. presented a one-dimensional model used to estimate the pH distribution during the electrokinetic process [17; 22]. Paz-Garcia et al. [19] presented a transport model based on the Poisson-Nernst-Planck system accounting for electroosmotic advection and water chemical equilibrium. Alshawabkeh and Acar [16; 17] developed a numerical solution for the equations describing reactive multi-component species transport under coupled hydraulic, electrical, and chemical concentration gradients. The finite element method (FEM) is used in space discretization and the finite difference method was used for time discretization. Predicted lead profile show excellent agreement with the pilot-scale test results on a kaolinite soil samples mixed with lead. This model couples electroosmotic consolidation with species transport, which is essential when electrokinetic-induced settlement is problematic.

An engineering design/analysis package for expedient field implementation of electrokinetic and electrochemical applications in environmental restoration requires the continued development of generalized mathematical formulation and the development of a comprehensive model for multi-component, reactive transport under coupled hydraulic, electric, and chemical gradients. The present work summarizes enhancements on the model developed by Alshawabkeh and Acar [16; 17]. A generalized model applicable to a soils contaminated with multiple metals under enhanced boundary conditions during electrokinetic processing is presented. The enhanced model is used to simulate electrokinetic cleanup of lead and copper contaminants at an Army Firing Range.

THEORETICAL FORMULATION

The conceptual model of the porous medium is as a solid framework of cation exchange surfaces with the pore space occupied by chemically reactive species in aqueous solution. Chemical species consist of N_i components which can react with each other to form N_j aqueous complexes and N_p precipitated solids. The choice of independent components is arbitrary, under the restriction that each component should represents one of the elements participating in the chemical system. Aqueous complexes and precipitates are defined as

function of the chosen components by a corresponding stoichiometric chemical reaction. Additionally, aqueous components and complexes may be adsorbed to the surface of N_{site} to form N_{si} adsorbed components and N_{sj} adsorbed complexes. Accordingly, the total number of aqueous species will be the sum of N_i aqueous components and N_j aqueous complexes. The total number of adsorbed species will be the sum of N_{si} and N_{sj}.

In the present formulation for modeling the transport of species under electric fields, c_i (i = 1, 2, …, N_i) refers to concentration of the i^{th} primary aqueous component (e.g., Pb^{2+}, Cu^{2+}), c_j (j = 1, 2, …, N_j) is the concentration of the complex j^{th} (e.g., $Pb(OH)^+$, $Cu(OH)^+$). Concentration of the i^{th} adsorbed component (e.g., Pb^{2+} -N_{site}, Cu^{2+} -N_{site}) is represented by s_i (i = 1, 2, …, N_{si}), while s_j (j = 1, 2, …, N_{sj}) is the concentration of the adsorbed j^{th} complex (e.g., $Pb(OH)^+$ -N_{site}, $Cu(OH)^+$ -N_{site}), and p_k (k = 1, 2, …, N_k) is the concentration of the precipitate k (e.g., $Pb(OH)_2(s)$, $Cu(OH)_2(s)$). Solute concentrations are expressed in units of moles/volume, adsorbed and precipitated concentrations are expressed in units of mass/mass of dry soil. The partial differential equations (PDEs) describing species transport are developed by applying the law of mass conservation to their fluxes. Transport PDEs (due to migration, advection and diffusion) of each component and complex aqueous species are combined to produce one PDE that describes transport of the total analytical concentrations of component species i (T_i), which are the primary dependent variables. This formulation forces the sum of the rates describing the change in species concentration due to chemical reactions to zero, i.e., $\sum R_{ij} = 0$, where R_{ij} is the rate of change in the concentration of species i due to the r^{th} chemical reaction, where r = 1, 2, …, N_T, and $N_T = N_x+N_s+N_y+N_p$. This will facilitate the operator splitting formulation for transport and geochemical reactions.

The differential equations describing transport of total analytical concentrations of the components species i are derived by applying the law of conservation to mass flux through a control volume. Mass fluxes are evaluated under electric, hydraulic, and chemical concentration gradients [17]. Accordingly the mass conservation equations are given by

$$n\frac{\partial T_i}{\partial t} = L(c_i) + \sum_{j=1}^{N_j} a_{ij} L\left(c_j\right) - \lambda_i T_i \quad ; \quad i = 1, 2, \ldots, N_i \qquad (3)$$

where n is the soil porosity, t is time, a_{ij} is the stoichiometric coefficient of the i^{th} aqueous component in the j^{th} complexed species, λ_i is the decay rate constant for the i^{th} aqueous component, assumed first order, and $L(c_i)$ is the flux term defined as:

$$L(c_i) = \nabla \cdot (D_i \nabla c_i + u_i c_i \nabla E + k_e c_i \nabla E + k_h c_i \nabla h) \qquad (4)$$

where D_i is the effective diffusion tensor of component i^{th}, u_i is the effective ionic mobility tensor of component i^{th}, k_e is the electroosmotic permeability tensor, k_h is the hydraulic conductivity tensor, E is the electric potential, and h is the hydraulic head. $L(c_j)$, the flux term for the aqueous complexes, is defined similarly. The total analytical concentrations of species i (T_i) are the sum of concentrations of all forms of species i and are given by,

$$T_i = c_i + \sum_{j=1}^{N_j} a_{ij} c_j + s_i + \sum_{j=1}^{N_j} a_{ij}^s s_j + \sum_{k=1}^{N_k} a_{ik}^p p_k \quad ; \quad i = 1, 2, \ldots, N_i \qquad (5)$$

where a_{ij}^{s} is the stoichiometric coefficient of the i^{th} aqueous component in the j^{th} adsorbed species, p_k is the concentration of the precipitate k^{th}, a_{ik}^{p} is the stoichiometric coefficient of the i^{th} aqueous component in the k^{th} precipitated species.

Charge Conservation

In the present model, ions transport under electric fields is assumed to be controlled by the electric neutrality of the free pore fluid.

$$\sum_{i=1}^{N_i} z_i c_i + \sum_{j=1}^{N_j} z_j c_j = 0 \quad (6)$$

Consequently, an equivalent positive and negative charge should pass through a unit volume in order to maintain zero net charge, assuming no electric capacitance of the porous medium. Application of Faraday's law to the flux terms defined in (4) results in the following charge conservation equation:

$$C_p \frac{\partial E}{\partial t} = F\left(\sum_{i=1}^{N_i} z_i L(c_i) + \sum_{j=1}^{N_j} z_j L\left(c_j\right)\right) \quad (7)$$

where z_i is the charge of the i^{th} component, z_j is the charge of the j^{th} complex, F is the Faraday's constant (96,485 C/mol), C_p is the electrical capacitance per unit soil volume ($F\ L^{-3}$). If the soil capacitance C_p is zero then equation (7) will result in:

$$\sum_{i=1}^{N_i} z_i L(c_i) + \sum_{j=1}^{N_j} z_j L\left(c_j\right) = 0 \quad (8)$$

which means that the net change in charge per unit volume of free pore fluid due to all species (components and complexes) transport is zero. Equation (8) is used to calculate the electrical potential distribution.

Geochemical Reactions

Transport of species under electric fields will be controlled by the nature and rates of geochemical reactions in the soil. Some base or acid produced by electrolysis reactions may be consumed in non-target reactions with the medium but convergence of the fronts creates locally sharp pH and concentration gradients and a challenge to robust geochemical modeling. Geochemical reactions that should be included in the geochemical model and will impact the transport include sorption, aqueous phase, redox, and precipitation/dissolution reactions. Recent developments showed that these reactions could be incorporated by a set of algebraic equations (for equilibrium reactions) and differential equations (for reaction kinetics). Mathematical treatment for some of these reactions is provided assuming instantaneous equilibrium, since aqueous chemical reaction rates are, generally, several order of magnitude faster than transport rates in most electrokinetic treatments [19].

Aqueous Phase Reactions

A set of nonlinear algebraic equations may be developed from mass balance considerations of the aqueous phase reactions. In this case, any complex j is the product of i^{th} reactant components, i.e.

$$c_j \rightleftarrows \sum_{i=1}^{N_i} a_{ij} c_i \quad ; \quad j=1,\ldots,N_j \quad (9)$$

where a_{ij} is the stoichiometric coefficient in complex j for component i (*mole j/mole i* or *mass j / mass i*). The law of mass action implies that

$$c_j = \frac{1}{K_j^{eq}} \prod_{i=1}^{N_i} c_i^{a_{ij}} \quad ; \quad j=1,\ldots,N_j \quad (10)$$

where K_j^{eq} is the equilibrium constant for aqueous reaction j^{th} described as a dissociation reaction. Precipitation/Dissolution reactions must be considered in the mass transport formulation because they can affect dramatically the electrokinetic efficiency. In precipitation reactions the stoichiometric reaction is defined similarly to aqueous equilibrium reaction,

$$p_k \rightleftarrows \sum_{i=1}^{N_i} a_{ik} c_i \quad ; \quad k=1,\ldots,N_k \quad (11)$$

where p_k is the chemical formula of precipitate k^{th}, a_{ik} is the stoichiometric coefficient of component i^{th} in precipitate k^{th} [mass/mass], and N_p is the number of precipitates. The existence of the precipitates species is conditional upon constituent solute(s) i^{th} concentrations exceeding the saturation index of k^{th}. The law of mass action is written as

$$\begin{cases} \prod_{i=1}^{N_i} c_i^{a_{ik}} = K_k^{sp} & p_k \neq 0 \\ \prod_{i=1}^{N_i} c_i^{a_{ik}} < K_k^{sp} & p_k = 0 \end{cases} \quad (12)$$

where K_k^{sp} is the solubility product equilibrium constant for precipitate k^{th} described as a dissolution reaction. The current model implementation neglects nonlinear effects of solute concentrations on ionic activity (e.g. Davies, Debye-Huckel, Pitzer or other model) and thus solubility index for precipitates. This limitation restricts model application to solutions of relatively low ionic strength and is one of our priority targets for relaxation.

Sorption Reactions

Sorption reactions will provide two sets of algebraic equations: one set for adsorbed components and another set for adsorbed complexes. Assuming instantaneous equilibrium in sorption reactions and linear isotherms,

$$\frac{\partial s_i}{\partial c_i} = K_{di} \quad (13)$$

where K_{di} is the distribution coefficient ($L^3 M^{-1}$) of species i^{th}. The same procedure could be used for adsorbed components or complexes. Simple isotherm sorption models ignore the potential effects of variations in pH, solute composition and ionic strength, redox potential, or processes such as competitive adsorption. Alternative, more robust (and complicated) sorption models include ion- or ligand-exchange, mass action models, and surface complexation models as described by several research groups [23-29]. The reader could refer

to some of these references for more rigorous treatment of sorption and other reactions such as redox.

Hydraulic Head and Soil Volume Change

Another variable that impacts reactive transport is the hydraulic gradients which will vary depending upon the compressibility of the porous medium. Since the process is used for remediation of soft cohesive soils, the compressibility of the medium will depend on the consolidation characteristics of the soil. Volume change in the soil medium due to consolidation is described by the following partial differential equation

$$m_v \gamma_w \frac{\partial h}{\partial t} = k_h \nabla^2 h + k_e \nabla^2 E \quad (14)$$

where m_v is the coefficient of volume compressibility ($L^2\ M^{-1}$) and γ_w is the unit weight of water ($M\ L^{-3}$). Solution of equation (14) will provide the hydraulic gradients that will be used in species transport. Equation (14) is dependent upon the soil parameters and also on the electric field intensity, which is dependent upon the species distribution.

Complete System of Equations

Nine sets of unknowns (T_i, c_i c_j, s_i, s_j, p_k, E, h, and σ^*) could be identified in this case for modeling reactive transport of species under electric fields. The required nine sets of equations for simulating the process are equations 3, 5-7, 10, 12, 2 equations of form 13 (one for components and another one for complexes), and 14. Equation sets 3, 7, and 14 are second order partial differential equation, thus three sets of boundary and initial conditions are needed. Boundary conditions for one-dimensional contaminant transport are derived from electrolysis reactions at the electrodes.

Electrolysis Reactions and Enhancements at Boundaries

Electrokinetic remediation can be adapted in a variety of options to enhance cleanup of the target contaminants and/or to accommodate site geology and geochemistry. In practice, much of this adaptation involves chemical conditioning or introduction of proper reactants at the electrodes. Thus, in terms of modeling, the major difference between these electrokinetic applications is the treatment of electrode boundary conditions. When inert electrodes (e.g., graphite) are used in groundwater, oxidation of water at the anode, equation (1), produces an acid front; while reduction of water at the cathode, equation (2), produces a basic front. Despite the water electrolysis of the pore solution is always likely to happen, the prevailing oxidation/reduction reactions at the electrodes might vary depending upon the chemical composition, pH, and the electrochemical potentials of these reactions. Multiple electrolysis reactions may occur at the cathode or anode depending on the water composition and electrochemical potential of each reaction. In general, the overall electrolysis (cell) reaction comprises two separated half-reactions: reduction at the anode and oxidation at the cathode. Consider the following half-cell reaction:

$$a_o \mathrm{O} + n e^- \rightleftarrows a_r \mathrm{R} \quad (15)$$

where O is the oxidized form, R is the reduced form, and a_o and a_r are the stoichiometric coefficients. The Gibbs free energy (G) of this cell reaction is given by

$$\delta G = \delta G^o + RT \ln \frac{[\mathrm{R}]^{a_r}}{[\mathrm{O}]^{a_o}} \quad (16)$$

where G^o is the standard free energy, R is the universal gas constant (8.3144 $J/K{\cdot}mol$), T is temperature (K), and the squared brackets represent activities. Since $G = -nFE$,

$$E = E^o - \frac{RT}{nF}\ln\frac{[\mathrm{R}]^{a_r}}{[\mathrm{O}]^{a_o}} \quad (17)$$

where E^o is the standard reduction potential versus the standard hydrogen electrode (*SHE*). Equation (17) is the Nernst Equation [30] and it provides the potential of the O/R electrode verses Natural Hydrogen Electrode (*NHE*) as a function of the activities of O and R. Equation (17) is useful for the identification of the electrolysis reactions to be expected at the electrode. The electrolysis reaction that has the highest positive redox potential, E, will occur at the cathode, while the electrolysis reaction with the most negative value of E will occur at the anode. These electrolysis reactions at the electrodes will drive continuous changes that will either enhance or retard the electrokinetic process.

Numerical Strategy

Three approaches were considered in the development of a numerical solution to differential and algebraic equations posed previously. The differential and algebraic equations approach (DAEA) consists of providing a solution to the mixed differential and algebraic equations in which the transport and reaction equations are solved simultaneously [27; 31; 32]. The direct substitution approach (DSA) consists of direct substitution of the algebraic chemical equilibrium equations into the differential transport equations to form a highly nonlinear system of partial differential equations [24; 26; 28; 33]. Finally, the sequential iteration approach (SIA) consists of iterating between the sequentially solved differential and algebraic equations [23; 25; 29]. The primary advantages of SIA over the other schemes (DAEA and DSA, which could be considered globally implicit schemes) is the lower computational memory requirements [34] and their greater flexibility to incorporate higher-order methods to accommodate advection-dominated systems [32], and in this case migration dominated transport. For the geochemical conditions to be simulated, DAEA and DSA offer no clear advantage to justify the memory overhead. At the same time, the two-steps SIA allows incorporating existing geochemical models in the developed system of transport rather than developing a specific geochemical model for transport under electric fields. The advantages and disadvantages of the schemes are discussed elsewhere [29; 32; 34]. The SIA is used in this study.

Model Application

The numerical model described here was developed in conjunction with basic and applied research on the electrokinetic recovery of lead from soils. Laboratory and field scale evaluation of the electrokinetic extraction of lead have been conducted using contaminated soils from a small arms firing range. The experimental study was conducted by Electrokinetics, Inc. (Baton Rouge, LA), in collaboration with the U.S. Army Engineers Waterways Experiment Station (WES), Vicksburg, Mississippi [9]. Soil samples were retrieved from a firing range situated along the bank of a small ephemeral /intermittent (usually dry) stream. Bullet fragments from several decades of operation littered the area, acting as a potential source of lead and copper contamination to surface and ground waters. Due to the low aqueous solubility of weathered lead, most fragments have remained in the bank and floodplain soils. Older small arms munitions have copper alloy jackets surrounding the lead alloy slug (solid tip of the projectile). Copper metal in electrical proximity to the lead induces galvanic (or cathodic) corrosion, accelerating the weathering and release of lead to the environment. Particulate lead also has been transported with other sediment along the creek with the seasonal flood events.

A laboratory pilot investigation was conducted in the WES Hazardous Waste Research Center (HWRC). The soil was retrieved from two depths at the contaminated firing range. A first set of samples was collected from the upper contaminated sand layer up to 30 cm depth. A second set of samples was then collected from the underlying, and relatively clean, clayey sandy layer up to a depth of 45 cm. The soil was placed in 208 L drums by a hauler. The drums were transported to WES on a flatbed truck. At WES, the soil was air dried and sieved through a 1/4 inch (6.35 mm) mesh to minimize the impact of discrete metal fragments on the investigation. However, appreciable amounts (about 8% by weight) of bullet fragments remained in the surface soil. The lower layer did not contain any fragments.

Soil mixing and homogenizing operations were carried in batches by addition of water (20% by weight of dry soil). Mixing was carried in a pool using a shovel. The soil was then transported to the testing area and was placed in a lined wooden container. The container inner dimensions were 76.2 cm width, 91.4 cm height, and 183 cm length (2.5 × 3 × 5 feet). A prefabricated, 80 mm thick, high density polyethylene (HDPE) liner was placed inside the containers as primary protection from any leakage. The soil was placed in layers inside the container and compacted with a hammer. The hammer used is a steel rod of 91.4 cm long, welded to a steal plate with a contact area of 15.2 cm × 15.2 cm. The gross weight of the hammer is 4.54 kg. The soil was compacted in seven layers. Each layer was compacted by dropping the hammer 800 times on top of the soil from a height of about 90 cm. Each layer thickness was about 10 cm after compaction. The natural stratification was replicated in the setup by first compacting 4 layers of the underlying clayey sand followed by three layers of the contaminated sandy soil. Electrodes were placed in wooden compartments that are 10 cm in width. Two cathode compartments were placed at the sides of the container, while one anode compartment was placed in the middle. This arrangement provided two cells each with a center to center cathode-anode spacing of about 87 cm. The soil was divided into two cells in order to compare the results and assure the quality and repeatability of data collected, as one of the cells was used for intermediate sampling.

Anode compartment had five, 5 cm diameter, holes for five graphite electrodes. Cathode compartment had a longitudinal slot to place galvanized mesh electrodes. A composite fabric supported by geotextile grid was nailed to the side of the electrode compartment in order to separate the electrolyte from soil and allow free water flow. Electrode compartments were filled with tap water up to the soil surface level. The electrodes were connected to the DC power supply and current of 1.2 A was applied. The current was divided in half by passing 0.6 A through each cell, rendering a current density of about 1.8 A/m^2 (cross-sectional area of the soil is 5500 cm^2). The test was processed for 9 months.

The electrochemical treatment was amended at the cathode by the injection of adipic acid to control pH. As mention before, control of the basic front will increase the solubility and thus the mobility of the target contaminants.

Initial chemical analysis was conducted on 36 randomly collected samples from the compacted layers. Initial and final sampling was conducted on both cells, whereas intermediate samples were collected every two weeks from one cell only. The intermediate samples were collected using 2.54 cm diameter tubes at 10 cm equally spaced locations between the anode and cathode. Final sampling was performed by slicing each cell into five horizontal layers. Each layer was divided into 8 longitudinal sections and 2 lateral sections of equal size. Prior to chemical analysis, the soil sample was oven dried, crushed with a mortar and a pistol, and sieved through 2.00 mm sieve. A riffle was also used for splitting the soil into equal portions. One gram samples were then taken from the riffled soil. EPA SW 846 Method 3051 was used for soil digestion. Inductively Coupled Plasma-Atomic

Emission Spectroscopy (ICP) was used for analysis of the leachate (EPA SW 846 Method 6010A). The soil was poorly sorted sand (an SP by the Unified Soil Classification System). Hydraulic conductivity of the soil was 9.8×10^{-5} cm/s; geotechnical properties of the soil are summarized in Table 1. Chemical analysis showed a mean lead concentration of 3041 mg/kg with a standard deviation of 887 mg/kg. Mean concentrations of other metals in the soil matrix included 589 mg/kg copper, 524 mg/kg calcium, and 96 mg/kg zinc.

Metal fragments impede the remediation process, acting as a significant internal source of contamination. Reactive transport of eight components (Pb^{2+}, Cu^{2+}, Ca^{2+}, NO_3^-, Cl^-, OH^-, A^{-2} and H^+) and four complexes ($Pb(OH)^+$, $Pb(OH)_2$, $Cu(OH)^+$, and $Cu(OH)_2$) are modeled in the present simulations. A^{-2} represents the adipate ion, $O_2C(CH_2)_4CO_2^{-2}$. The system of differential equations required to implement the code for this case of lead extraction includes eight transport equations, one volume change equation and one charge conservation. Initial concentrations (e.g., total lead and copper concentrations), soil parameters (e.g., hydraulic conductivities, electroosmotic permeability), and boundary conditions must be defined. Table 2 summarizes all initial concentration of components used in the present simulations.

Only the boundaries represented by the anode ($x = 0$) and cathode ($x = L$) need be defined in the one-dimensional simulations presented here. Hydraulic head gradient is set to zero, consistent with the experimental setup, which results in the following boundary conditions for equation (18):

$$h|_{x=0} = h|_{x=L} = 0 \quad (18)$$

Boundary conditions for charge conservation equation are developed from the current value at the boundary. The constant current applied through the experiment requires the following transport boundary conditions:

$$\left[F \sum_{i=1}^{N_i} z_i D_i \frac{\partial c_i}{\partial x} + F \sum_{j=1}^{N_j} z_j D_j \frac{\partial c_j}{\partial x} - \sigma^* \frac{\partial E}{\partial x} \right]_{x=0} = 0 \quad ; \quad E|_{x=L} = 0 \quad (19)$$

Boundary conditions for the given species transport equation are evaluated based on the flux of each species at the cathode and the anode. There are two components of mass fluxes at the electrode, one is due to water advection (advective component, including electroosmosis since there is no hydraulic gradient) and the other is due to electrolysis (current component). The mass fluxes of any species (component or complex) at the cathode and at the anode are given by:

$$\left| -D_i \frac{\partial c_i}{\partial x} + \nu_i c_i + \sum_{j=1}^{N_j} a_{ij} \left[-D_j \frac{\partial c_j}{\partial x} + \nu_j c_j \right] \right|_{x=0} = T_i \mathbf{J}_w + \frac{I_i}{z_i F} + \sum_{j=1}^{N_j} \frac{a_{ij} I_j}{z_j F} \quad (20)$$

$$\left| -D_i \frac{\partial c_i}{\partial x} + \nu_i c_i + \sum_{j=1}^{N_j} a_{ij} \left[-D_j \frac{\partial c_j}{\partial x} + \nu_j x_j \right] \right|_{x=L} = T_i \mathbf{J}_w + \frac{I_i}{z_i F} + \sum_{j=1}^{N_j} \frac{a_{ij} I_j}{z_j F} \quad (21)$$

where $\mathbf{J}_w$ is the advective flux at the electrodes, I_i and I_j are the partial current densities, and the v_i, is defined by:

$$v_i = -(u_i - k_e)\frac{\partial E}{\partial x} - k_h \frac{\partial h}{\partial x} \quad (22)$$

and v_j is defined similarly for the complexes. The partial current density of a component or a complex is the percentage of the total current that is employed in production the specific component or complex due to electrolysis reactions. The partial current densities are evaluated based on the electrolysis reactions of each component and complex. For example, if only water electrolysis is occurring at the electrodes, then at the anode the partial current densities are 1.0 for H^+ and zero for all other species. Similarly at the cathode the partial current densities are 1.0 for OH^- and zero for all other species.

RESULTS AND DISCUSSION

Figure 1 shows the transport of the acid front developed at the anode. The pH profile does not show an increase of the pH value at the cathode. The adipic acid added to the cathode compartments neutralized the water electrolysis reaction at this end of the setup and prevented the development of a high pH zone at the cathode.

Figure 2 shows comparisons of the experimental and predicted pH profiles for the first pilot-scale test. The comparisons indicate that the advance of pH front is overestimated by the model.

The model results show that predicted breakthrough of pH front at the cathode occurs in 14 weeks (98 days). On the other hand, the experimental results do not show a breakthrough of the acid front even after 270 days of processing. A similar behavior is noted in prediction of lead and copper transport. This overestimation of transport of ions could be related to many reasons. Rate of transport of charged particles is a function of the electric gradient ion mobility and pore fluid chemistry. An overestimate of ion transport could be due to overestimate of electric field strength, overestimate of effective ionic mobility, and/or improper handling of soil pore fluid chemistry. Comparisons of predicted and measured electric gradients (Figure 3) show that the model underestimates the electric potential and electric gradient. This result is due to the fact that the predicted electric conductivity of the pore solution is higher than the measured one. This will lead to the other reason for overestimating the rate of acid transport, which is the effective ionic mobility of the species.

As described earlier, the effective ionic mobility is assumed equal to the ionic mobility at infinite dilution multiplied by soil porosity and soil tortuosity. Proper evaluation of porosity and tortuosity is important for modeling; yet, the critical factor is the use of ionic mobility coefficients at infinite dilution. It is established in electrochemistry that ionic mobilities are dependent on the ionic strength of the solution. Thus, the use ionic mobilities at infinite dilution for measuring the effective ionic mobilities, which is considered valid, needs to be further investigated. However, since the resultsoverestimated acid transport rates and due to increased interest of electrochemical processing of soil, it is recommended that more basic research is needed to better understand ionic migration in soils.

Other important factor that will impact acid transport is pore fluid and soil chemistry. Soil buffer capacity could limit the acid advance. However, the soil used in the pilot-scale experiments is a silty sand soil with limited buffer capacity. Presence of bullet fragments and other species could result in some buffer capacity of the soil. The efficiency of electrolysis reaction at the anode also needs to be considered. It is expected that electrolysis reactions might occur at less than 100% efficiency. This defines the boundary condition for the acid transport. Water oxidation at the anode is assumed to occur at 100% efficiency. This

might be another reason for overestimation of the rate of advance of the acid front. Efficiencies less than 100% could be used for electrolysis reactions at the electrodes. Yet, these values will be estimated and might not represent real life conditions.

Figure 4 shows predicted lead profiles in the pilot-scale study. Predicted profiles indicate that full extraction of lead could be achieved in 100 days (about 3 to 4 months). On the other hand, experimental results showed that it took about 9 months to reduce lead concentration to less than 300 mg/kg.

Figure 5 shows comparison between predicted and measured lead profiles in the soil after 2 and 14 weeks of processing. Predicted profiles show reasonable agreement with experimental results. However, comparisons after 15 weeks show that the model overestimates lead transport. Similar to the advance of the acid front, predicted rates of lead transport are faster than measured ones. This again will question the use of lead ionic mobility at infinite dilution for estimation of lead effective ionic mobility in soils. The more significant factor in predicting lead transport is the geochemistry and impact of bullet fragments on lead concentration. Initial soil pH was around 4. During processing, predicted and measured pH profiles clearly show the drop in pH to around 2, especially near the anode. This will lead to lead dissolution, desorption, and consequently migration. The two important factors in realistic prediction of lead transport are (a) dissolution of lead from bullet fragments and precipitates and (b) the kinetics of lead dissolution. The predicted transport did not account for presence of 8% bullet fragments. These fragments contain significant amount of lead, copper, and zinc, which will leach in time with the advance of the acid from the anode. These fragments will act as a continuous source of lead. This is the major reason for the differences between predicted and measured lead profiles. The predicted profiles show cleanup of lead to minimal concentrations across the sample. The measured concentrations show a steady-state final lead concentration in the soil in the range of 200 to 500 mg/kg. These concentrations could be the equilibrium values of lead in solution due to its leaching from bullet fragments. The significance of the bullet fragments is observed in the case of copper transport.

Figure 6a displays predicted copper profiles while Figure 6b displays measured final copper profiles. The predicted profiles show a decrease in copper concentration with time and complete extraction after 14 weeks. The measured final copper profiles show increase in copper concentrations near the cathode. In fact the measured final copper concentrations were higher than the initial concentrations. This increase is directly related to its leaching from the bullet fragments which was not incorporated in the model predictions. One method to handle leaching of contaminants from bullet fragments is to assume a constant source in the soil. This however will require a more elaborate work on the geochemistry involved. Lead, copper, and zinc leaching rate kinetics will be of significant importance in such enhancement. An elaborate geochemical code is needed for more realistic prediction of the process. Furthermore, the results suggest that there is a need for better understandings of the basic physicochemical soil properties.

SUMMARY AND CONCLUSIONS

The paper presents a generalized model for simulating contaminants transport and extraction from soils by electric fields. The model is able to simulate enhanced application of the process by modifying the boundary conditions. The model is applied for the case of lead and copper extraction from a contaminated soil sample collected from an Army Firing Range site by enhanced electrokinetic processing. While model performance was realistic in the first few weeks of processing, it showed that further understanding of physicochemical and

geochemical processes is needed for proper simulation of such a complicated process in a "real world" soil. These understandings include (a) verifying existing methods for estimating effective ionic mobilities in soils and/or development of other theoretical or experimental procedures for accurate evaluation of effective ionic mobilities in soils at variable pH and ionic strength conditions, (b) the geochemical sub-model used in this study is a limited sub-model that accounts for basic geochemical reactions, such as precipitation dissolution and/or complexation. This sub-model is shown to be appropriate for modeling lab experiments where synthetic soils are mixed with contaminants. This study showed that such basic geochemical sub-model has limitations in predicting geochemistry during enhanced EK application in real contaminated soil. The model also showed that kinetics of geochemical reactions, such as metals dissolution/leaching and redox reactions might be significant for realistic prediction of enhanced electrokinetic extraction of metals in real world applications.

Acknowledgments

Partial support of the work described is provided through Award Number P42ES017198 from the National Institute of Environmental Health Sciences. The content is solely the responsibility of the authors and does not necessarily represent the official views of the National Institute of Environmental Health Sciences or the National Institutes of Health.

REFERENCES

[1]. Lageman R, Pool W, Seffinga G. Electro-reclamation: Theory and practice. Chemistry and Industry. 1989:585–590.

[2]. Shapiro A, Renaud P, Probstein RF. Preliminary studies on the removal of chemical species from saturated porous media by electroosmosis. Physicochemical Hydrodynamics. 1989; 11:785–802.

[3]. Hamed J, Gale RJ. Pb (II) removal from kaolinite by electrokinetics. Journal of Geotechnical Engineering-Asce. 1991; 117:241–270.

[4]. Probstein RF, Hicks RE. Removal of contaminants from soils by electric fields. Science. 1993; 260:498–503. [PubMed: 17830427]

[5]. Runnells DD, Wahli C. In situ electromigration as a method for removing sulfate, metals, and other contaminants from ground water. Ground Water Monitoring & Remediation. 1993; 13:121–129.

[6]. Lageman R. Electroreclamation. Applications in the Netherlands. Environmental Science & Technology. 1993; 27:2648–2650.

[7]. Acar YB, Alshawabkeh AN. Principles of electrokinetic remediation. Environmental Science & Technology. 1993; 27:2638–2647.

[8]. Acar YB, Alshawabkeh AN. Electrokinetic remediation .1. Pilot-scale tests with lead-spiked kaolinite. Journal of Geotechnical Engineering-Asce. 1996; 122:173–185.

[9]. Alshawabkeh AN, Bricka RM, Gent DB. Pilot-scale electrokinetic cleanup of lead-contaminated soils. Journal of Geotechnical and Geoenvironmental Engineering-ASCE. 2005; 131:283–291.

[10]. Kim DH, Ryu BG, Park SW, Seo CI, Baek K. Electrokinetic remediation of Zn and Ni-contaminated soil. Journal of Hazardous Materials. 2009; 165:501–505. [PubMed: 19010593]

[11]. Ryu BG, Park SW, Baek K, Yang JS. Pulsed Electrokinetic Decontamination of Agricultural Lands around Abandoned Mines Contaminated with Heavy Metals. Separation Science and Technology. 2009; 44:2421–2436.

[12]. Ryu BG, Yang JS, Kim DH, Baek K. Pulsed electrokinetic removal of Cd and Zn from fine-grained soil. Journal of Applied Electrochemistry. 2010; 40:1039–1047.

[13]. Acar YB, Gale RJ, Alshawabkeh AN, Marks RE, Puppala S, Bricka M, Parker R. Electrokinetic remediation: Basics and technology status. Journal of Hazardous Materials. 1995; 40:117–137.

[14]. Puppala SK, Alshawabkeh AN, Acar YB, Gale RJ, Bricka M. Enhanced electrokinetic remediation of high sorption capacity soil. Journal of Hazardous Materials. 1997; 55:203–220.

[15]. Shapiro AP, Probstein RF. Removal of contaminants from saturated clay by electroosmosis. Environmental Science & Technology. 1993; 27:283–291.

[16]. Alshawabkeh AN, Acar YB. Removal of contaminants from soils by electrokinetics: A theoretical treatise. Journal of Environmental Science and Health, Part A. 1992; 27:1835–1861.

[17]. Alshawabkeh AN, Acar YB. Electrokinetic remediation .2. Theoretical model. Journal of Geotechnical Engineering-Asce. 1996; 122:186–196.

[18]. Jacobs RA, Sengun MZ, Hicks RE, Probstein RF. Model and experiments on soil remediation by electric fields. Journal of Environmental Science and Health, Part A. 1994; 29:1933–1955.

[19]. Paz-García JM, Johannesson B, Ottosen LM, Ribeiro AB, Rodríguez-Maroto JM. Modeling of electrokinetic processes by finite element integration of the Nernst-Planck-Poisson system of equations. Separation and Purification Technology. 2011; 79:183–192.

[20]. Haran BS, Popov BN, Zheng G, White RE. Mathematical modeling of hexavalent chromium decontamination from low surface charged soils. Journal of Hazardous Materials. 1997; 55:93–107.

[21]. Jacobs RA, Probstein RF. Two dimensional modeling of electroremediation. AIChE journal. 1996; 42:1685–1696.

[22]. Acar YB, Alshawabkeh AN, Gale RJ. Fundamental aspects of electrokinetic remediation of soils. Waste Management. 1993; 13:513.

[23]. Kirkner D, Jennings A, Theis T. Multisolute mass transport with chemical interaction kinetics. Journal of Hydrology. 1985; 76:107–117.

[24]. Jennings AA, Kirkner DJ, Theis TL. Multicomponent equilibrium chemistry in groundwater quality models. Water Resources Research. 1982; 18:1089–1096.

[25]. Kirkner DJ, Theis TL, Jennings AA. Multicomponent solute transport with sorption and soluble complexation. Advances in water resources. 1984; 7:120–125.

[26]. Lewis FM, Voss CI, Rubin J. Solute transport with equilibrium aqueous complexation and either sorption or ion exchange: Simulation methodology and applications. Journal of Hydrology. 1987; 90:81–115.

[27]. Lichtner PC. Continuum model for simultaneous chemical reactions and mass transport in hydrothermal systems. Geochimica et Cosmochimica Acta. 1985; 49:779–800.

[28]. Valocchi AJ, Street RL, Roberts PV. Transport of ion-exchanging solutes in groundwater: Chromatographic theory and field simulation. Water Resources Research. 1981; 17:1517–1527.

[29]. Yeh GT, Tripathi VS. A model for simulating transport of reactive multispecies components: model development and demonstration. Water Resources Research. 1991; 27:3075–3094.

[30]. Bard, A.; Faulkner, L. Electrochemical methods: fundamentals and applications. John wiley & Sons; Canada: 1980.

[31]. Miller C, Benson L. Simulation of solute transport in a chemically reactive heterogeneous system: Model development and application. Water Resources Research. 1983; 19:381–391.

[32]. Steefel CI, Lasaga AC. A coupled model for transport of multiple chemical species and kinetic precipitation/dissolution reactions with applications to reactive flow in single phase hydrothermal systems. American Journal of Science. 1994; 294:529–592.

[33]. Rubin J. Transport of reacting solutes in porous media: Relation between mathematical nature of problem formulation and chemical nature of reactions. Water Resources Research. 1983; 19:1231–1252.

[34]. Yeh G, Tripathi V. A critical evaluation of recent developments in hydrogeochemical transport models of reactive multichemical components. Water Resources Research. 1989; 25:93–108.

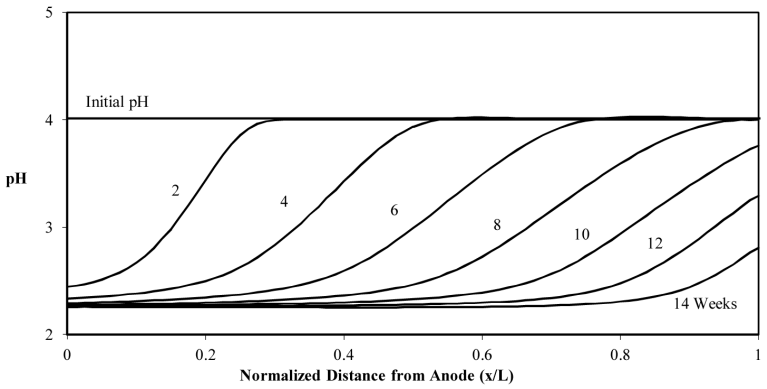

FIGURE 1.
Predicted pH profiles across the pilot-scale sample

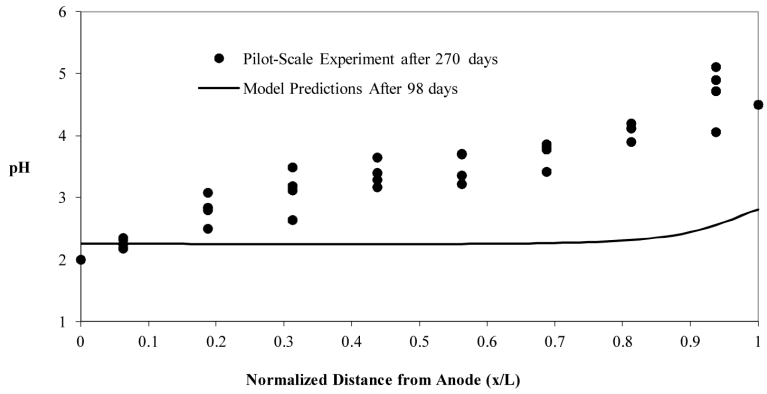

FIGURE 2.

Comparisons between predicted pH profile after 98 days and experimental pH profile after 270 days showing the model predictions overestimate acid transport rates

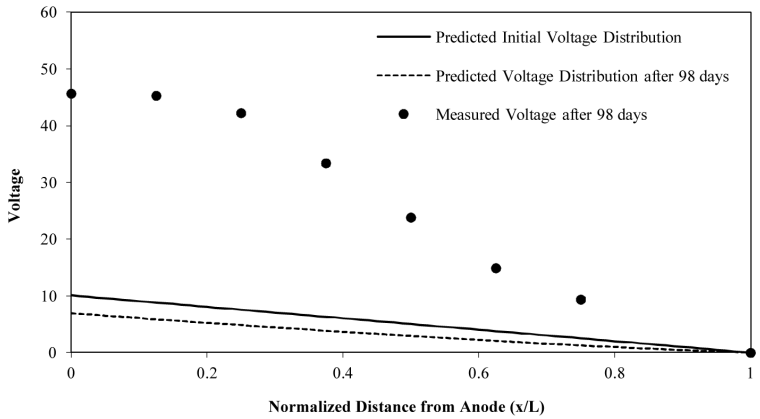

FIGURE 3.
Comparisons between predicted and measured voltage profiles across the soil sample

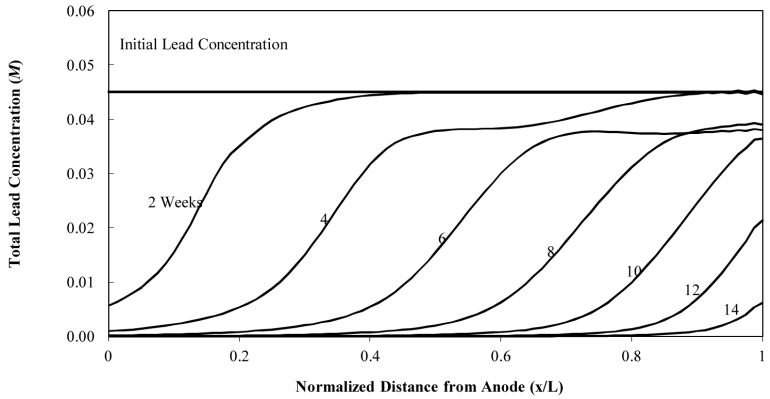

FIGURE 4.
Predicted Lead Transport in Two Weeks Intervals

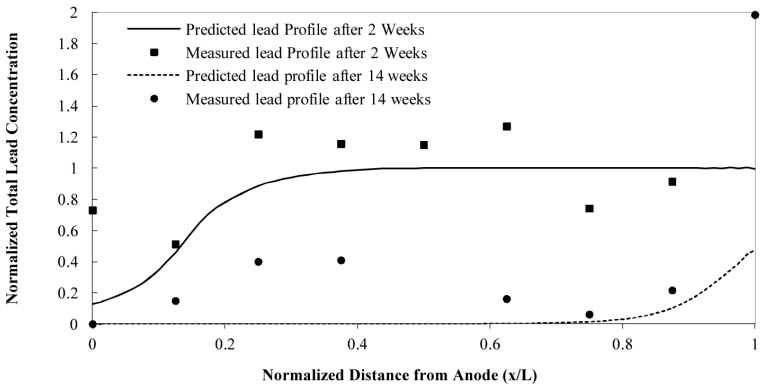

FIGURE 5.
Comparisons between Predicted and Measured Lead Profiles after 2 and 14 Weeks

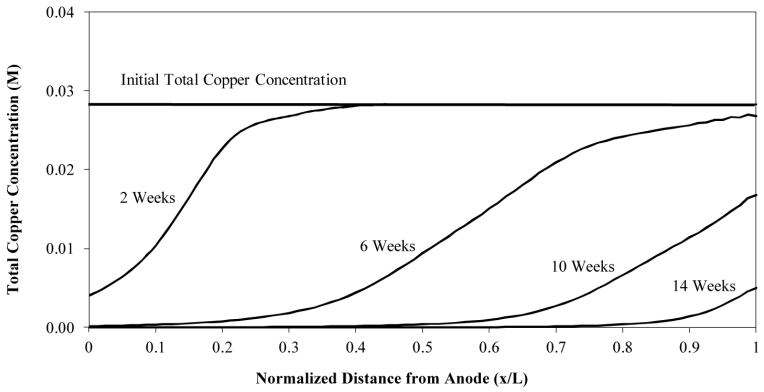

FIGURE 6a.
Predicted Cu Transport in the Pilot-scale Test

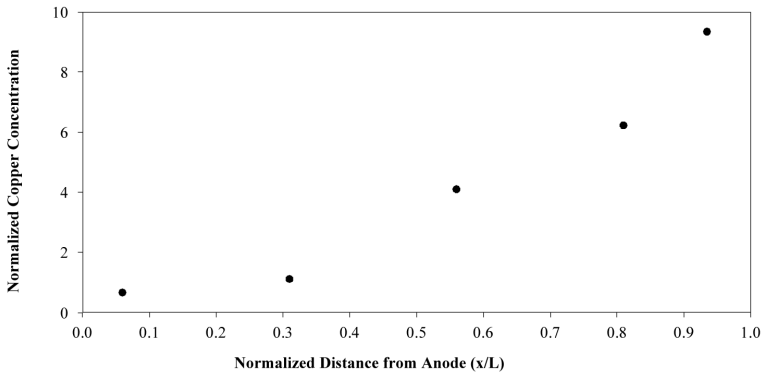

FIGURE 6b.
Measured Total Cu Concentration after 39 Weeks of Processing

TABLE 1

Soil Geotechnical Properties

Depth below surface	Contaminated Sandy soil	Underlying clayey sand
Initial water content w_i (%)	18.2	20.2
Initial degree of saturation S (%)	56	66
Liquid Limit	-	22.6
Plastic Limit	-	14
Plasticity index	-	8.6
Specific Gravity (G_s)	2.61	2.64
γ_d (kN/m^3)	13.8	14.5
Porosity (n)	0.46	0.44
Void Ratio (e)	0.85	0.79
Permeability (cm/s)	9.8×10^{-5}	2×10^{-7}
Unified Soil Classification System	SP	SC

TABLE 2

Concentration of Components Used in Modeling Pilot-Scale Study

Parameter	Initial Concentration (M)
Pb^{2+}	0.0449
Cu^{2+}	0.0283
Ca^{2+}	0.0400
NO_3^-	0.1120
Cl^-	0.1130
OH^-	1×10^{-4}
A^{-2}	0
H^+	1×10^{-10}